Int. J. Solids Structures, 1972, Vol. 8, pp. 1169 to 1183. Pergamon Press. Printed in Great Britain

INCREMENTAL CONSTITUTIVE LAWS AND THEIR ASSOCIATED FAILURE CRITERIA WITH APPLICATION TO PLAIN CONCRETE

M. D. COON and R. J. EVANS

Department of Civil Engineering, University of Washington, Seattle 98105

Abstract—A time independent incremental constitutive law corresponding to hypoelasticity is examined with particular reference to its description of failure. Material constants applicable to plain concrete are determined and the resulting law is shown to describe the behavior up to and including failure for both triaxial and combined torsion and compression loading.

1. INTRODUCTION

THE time independent or short term mechanical behavior of solids is most often described by using linear elasticity for small loads together with a yield criteria and plastic flow rule for large loads. This description is simple enough mathematically to allow the solution of many boundary value problems and is adequate to describe the most important features of the short term mechanical behavior of many metals. There are other materials, however, such as plain concrete, rock and engineering soils for which the measured short term uniaxial stress–strain relation has essentially no linear range and for which the slope of the stress–strain diagram is continuous up to and including "failure". The development of a single constitutive law to describe the entire response during loading would be of considerable value. The main purpose of this paper is to utilize an incremental description to develop such a constitutive law.

A time independent incremental constitutive law by which an increment of stress is related to the stress and an increment of strain was introduced by Truesdell [1], who called this kind of behavior hypoelastic. The relationship of hypoelasticity to plasticity has been investigated by Truesdell [2] and by Green [3, 4], who attempted to retain the features of plasticity as related to the deformation of metals.

The application of such a constitutive relation to frictional materials appears to have certain advantages. That the nonlinear character of the response can be predicted has been shown by Coon and Evans [5] who made use of available experimental data for sands to show that the *recoverable* response of cohesionless soils could be described by a first order hypoelastic law. These ideas are extended here in that the hypoelastic law is used to describe total response during loading up to and including failure. It is shown that, by proper selection of constants, the essential features of the short term response of frictional materials may be predicted. The law contains a failure or stability criteria and this is developed and compared with the concept of yield and its associated flow rule. The criterion is then used to investigate the stability of triaxial states of loading. Finally, availab[l] experimental data for plain concrete is fitted by the hypoelastic law, and it is shown [t]hat the salient features of the behavior from zero load to failure are predicted.

2. HYPOELASTIC BEHAVIOR

A constitutive relationship of the form

$$F(\sigma, e, \dot{\sigma}, \dot{e}) = 0 \tag{1}$$

provides a general representation for time independent incremental behavior provided it is homogeneous in time. Bearing in mind the subsequent application of this work to problems involving such materials as soils, rock and plain concrete for which nonlinear behavior occurs for small deformations, only small quasistatic deformations are considered. Then σ and e represent the classical stress and strain tensors, respectively; the dot represents differentiation with respect to a scalar parameter and F is a tensor function.

In order to extract a particular equation from the general form (1), several assumptions about the material behavior will be made. Following Truesdell, it will be assumed that an increment of stress depends only on the stress state and the increment of strain; further, it will be assumed that the increment of stress depends linearly on the increment of the strain. With these assumptions, equation (1) takes the form

$$\mathrm{d}\sigma_{ij} = A_{ijkl}(\sigma_{ij})\,\mathrm{d}e_{kl}. \tag{2}$$

If, in addition, it assumed that the material behavior is isotropic and that stress appears in equation (2) only to the first power, then the most general form for the material property tensor A_{ijkl} is (see [1])

$$\begin{aligned} A_{ijkl} = {} & (a_{01}+a_{11}\sigma_{rr})\delta_{ij}\delta_{kl}+\tfrac{1}{2}(a_{02}+a_{12}\sigma_{rr})(\delta_{ik}\delta_{jl}-\delta_{jk}\delta_{il}) \\ & +a_{13}\sigma_{ij}\delta_{kl}+\tfrac{1}{2}a_{14}(\sigma_{jk}\delta_{li}+\sigma_{jl}\delta_{ki}+\sigma_{ik}\delta_{lj}+\sigma_{il}\delta_{kj})+a_{15}\sigma_{kl}\delta_{ij} \end{aligned} \tag{3}$$

and the constitutive law has the explicit form:

$$\begin{aligned} \mathrm{d}\sigma_{ij} = {} & a_{01}\dot{e}_{kk}\delta_{ij}+a_{02}\dot{e}_{ij}+a_{11}\sigma_{pp}\dot{e}_{kk}\delta_{ij} \\ & +a_{12}\sigma_{kk}\dot{e}_{ij}+a_{13}\sigma_{ij}\dot{e}_{kk}+a_{14}(\sigma_{jk}\dot{e}_{ik}+\sigma_{ik}\dot{e}_{jk}) \\ & +a_{15}\sigma_{kl}\dot{e}_{kl}\delta_{ij}. \end{aligned}$$

The behavior described by equation (3) which is, by definition isotropic, exhibits stress induced anisotropy as evidenced by the last three terms in equation (3). This same phenomenon occurs in most nonlinear isotropic behavior (e.g. [6]).

The material behavior to be studied now revolves around the seven material properties a_{01}–a_{15}. Note that if all material property constants other than a_{01} and a_{02} are eliminated, then the representation is that of Hooke's law with the additional freedom that an initial stress can be prescribed for the zero strain state. The general conditions under which equation (2) represents elastic behavior, i.e. when the equations can be integrated to allow total stress to be related to total strain, has been investigated by Coon and Evans [5] and the five sets of conditions which must be satisfied simultaneously are as follows:

$$\begin{aligned} a_{14} &= 0 \\ a_{12}(3a_{11}+a_{12}) &= 0 \\ a_{12}a_{15} &= 0 \\ a_{15}(3a_{11}+a_{15}) &= 0 \\ 3a_{01}a_{12}+a_{02}(a_{12}-a_{13}) &= 0. \end{aligned} \tag{4}$$

In addition, the requirement

$$a_{13} = a_{15} \tag{5}$$

guarantees that the behavior is hyperelastic.

For any combination of material properties which do not satisfy equations (4) and (5), stress and strain will depend on the loading path. If one searches for a failure or yield criterion, one seeks a stress state for which incremental deformations may occur with no change in stress. From equation (2) such a condition is

$$A_{ijkl}\,de_{kl} = 0. \tag{6}$$

Equation (6) is satisfied when

$$\det A_{ijkl} = 0. \tag{7}$$

Equation (7) describes a stress condition for failure. This condition will, however, be accompanied by a state of strain and, hence, displacement. The initial assumption of small displacement gradients places a restriction on failure states which must be satisfied in addition to equation (7). To facilitate the calculation of this determinant, it is convenient to align the coordinates with the principal directions of stress. The determinant in equation (6) then takes on the form

$$\begin{vmatrix} K_1 & K_{12} & K_{13} & 0 & 0 & 0 \\ K_{21} & K_2 & K_{23} & 0 & 0 & 0 \\ K_{31} & K_{32} & K_3 & 0 & 0 & 0 \\ 0 & 0 & 0 & K_4 & 0 & 0 \\ 0 & 0 & 0 & 0 & K_5 & 0 \\ 0 & 0 & 0 & 0 & 0 & K_6 \end{vmatrix} = 0 \tag{8}$$

where

$$\begin{aligned} K_{ij} &= a_{01}+a_{11}I_1+a_{13}\sigma_i+a_{15}\sigma_j \quad \text{for } i \neq j \quad \text{and} \quad i,j = 1,2,3 \\ K_i &= a_{01}+a_{02}+(a_{11}+a_{12})I_1+(a_{13}+2a_{14}+a_{15})\sigma_i \quad \text{for } i = 1,2,3 \\ K_4 &= \rho+a_{14}(I_1-\sigma_1) \\ K_5 &= \rho+a_{14}(I_1-\sigma_2) \\ K_6 &= \rho+a_{14}(I_1-\sigma_3) \end{aligned}$$

where $I_1 = \sigma_1+\sigma_2+\sigma_3$, $\rho = a_{02}+a_{12}I_1$, and σ_1, σ_2 and σ_3 are the principal stresses. The expansion of equation (8) leads to

$$\begin{aligned} &(\rho\{-3a_{13}a_{15}J_2+[3a_{01}+a_{02}+(3a_{11}+a_{12}+a_{13}+a_{15})I_1]\} \\ &\quad +2a_{14}\{\rho^2 I_1+2\rho I_1(a_{01}+a_{11}I_1)+(2I_1^2/3-J_2)[a_{14}(a_{01}+a_{11}I_1) \\ &\quad +\rho(a_{13}+a_{14}+a_{15})]+(I_3/3-I_1J_2/2)[2a_{14}(3a_{13}+2a_{14}+3a_{15}) \\ &\quad +6a_{13}a_{15}]-a_{13}a_{15}[I_1^3/3+I_1J_2-I_3]\})K_4K_5K_6 = 0 \end{aligned} \tag{9}$$

where

$$I_2 = \sigma_1^2+\sigma_2^2+\sigma_3^2$$
$$J_2 = I_2 - I_1^2/3 \tag{10}$$
$$I_3 = \sigma_1^3+\sigma_2^3+\sigma_3^3.$$

The failure criteria of equation (9) can be interpreted geometrically as a surface in principal stress space. Actually there are two surfaces involved, the first resulting from the product of $K_4K_5K_6$ which is pyramidal, while the second results from the determinant of K_{ij} where $i,j = 1,2,3,(1 \neq j)$ and K_i where $i = 1,2,3$, which is a curved surface in stress space. The actual failure surface is the one which encloses the smallest region containing the origin.

When $a_{14} = 0$, the failure surface is given by

$$(a_{02}+a_{12}I_1)\{-3a_{13}a_{15}J_2+(a_{02}+a_{12}I_1)[3a_{01}+a_{02}+(3a_{11}+a_{12}+a_{13}+a_{15})I_1]\} = 0. \tag{11}$$

Equation (11) again consists of two surfaces, one being a mean stress sensitive version of the von Mises' yield criterion and the other a plane cut-off perpendicular to the hydrostatic stress axes. The mean stress sensitive version of the Mises' yield criterion has been proposed by Drucker and Prager [7] for use in soil mechanics.

The determinant of equation (7) can be interpreted as a condition of stability as well as that of failure. Hill [8] has shown that this determinant provides a limiting condition for the invertibility of equation (2) when it represents elastic behavior and has considered this as a material stability condition.

Whatever the interpretation of equation (9), as a criteria of stability, failure or plasticity, it is clear that there is a class of deformations associated with these stresses analogous to a plastic flow rule. When the plastic yield criterion is the incremental plastic strain potential [9], then the strain increment vector is normal to the yield surface and principal directions of stress and strain rate coincide. Looking at the determinant of equation (8) it is clear that on the pyramidal part of the failure surface the principal directions of incremental strain will not coincide with those of principal stress. There is some indication that principal directions of stress and strain rate do not coincide for frictional materials [10]. On that part of the failure surface which results from K_{ij}, where $i,j = 1,2,3$ $(i \neq j)$ and K_i, where $i = 1,2,3$, the principal direction of stress and strain rate do coincide; however there is no assurance of normality. The increments of strain are related by

$$\frac{de_2}{de_1} = \frac{-K_{11}K_{23}+K_{21}K_{13}}{K_{12}K_{23}-K_{22}K_{13}}$$
$$\frac{de_3}{de_1} = \frac{-K_{12}K_{21}+K_{11}K_{22}}{K_{12}K_{23}-K_{22}K_{13}}. \tag{12}$$

There are indications that the normality condition is not satisfied for frictional materials [11] and theoretical investigations of this kind of behavior have been made by Palmer [12] and Mroz [13]. Because of the lack of both normality and coincidence of principal directions, the standard bounding theorems of plasticity cannot be applied directly to this material.

3. TRIAXIAL BEHAVIOR

Triaxial states of stress will be considered here in order to illustrate the implications of the previous section and also because the results will be of later use.

Let

$$\sigma_{ij} = \begin{vmatrix} \sigma & 0 & 0 \\ 0 & p & 0 \\ 0 & 0 & p \end{vmatrix} \tag{13}$$

where σ is the axial stress and p is the lateral pressure. Combining equations (3), (8) and (13), one obtains

$$\begin{vmatrix} K_1 & K_{12} & K_{12} & 0 & 0 & 0 \\ K_{21} & K_2 & K_{23} & 0 & 0 & 0 \\ K_{21} & K_{23} & K_2 & 0 & 0 & 0 \\ 0 & 0 & 0 & K_4 & 0 & 0 \\ 0 & 0 & 0 & 0 & K_5 & 0 \\ 0 & 0 & 0 & 0 & 0 & K_4 \end{vmatrix} = 0 \tag{14}$$

where

$$\begin{aligned} K_1 &= a_{01}+a_{02}+(a_{11}+a_{12})I_1+(a_{13}+2a_{14}+a_{15})\sigma \\ K_2 &= a_{01}+a_{02}+(a_{11}+a_{12})I_1+(a_{13}+2a_{14}+a_{15})p \\ K_{12} &= a_{01}+a_{11}I_1+a_{13}\sigma+a_{15}p \\ K_{21} &= a_{01}+a_{11}I_1+a_{13}p+a_{15}\sigma \\ K_{23} &= a_{01}+a_{11}I_1+(a_{13}+a_{15})p \\ K_4 &= a_{02}+a_{12}I_1+2a_{14}p \\ K_5 &= a_{02}+a_{12}I_1+a_{14}(\sigma+p) \end{aligned} \tag{15}$$

where

$$I_1 = \sigma+2p.$$

There are four cases for which the determinant in equation (14) is zero, each having its own mode of failure. These conditions and associated flow modes are

$$\begin{aligned} &\text{(a) } K_2-K_{32} = 0 : \mathrm{d}e_{ij} = 0 \text{ except } \mathrm{d}e_2 = -\mathrm{d}e_3, \\ &\text{(b) } K_1K_2+K_1K_{23}-2K_{12}K_{21} = 0 : \mathrm{d}e_2 = \mathrm{d}e_3, \frac{\mathrm{d}e_1}{\mathrm{d}e_2} = \frac{-K_1}{K_{12}}, \\ &\text{(c) } K_4 = 0 : \mathrm{d}e_{ij} = 0 \text{ except } \mathrm{d}e_{12}, \\ &\text{(d) } K_5 = 0 : \mathrm{d}e_{ij} = 0 \text{ except } \mathrm{d}e_{23}. \end{aligned} \tag{16}$$

The modes of failure for these various conditions are obtained by substituting failure conditions into (6). From (15) it may be seen that (16a) and (16d) are identical and hence three possible failure modes exist. On substitution from (15), these become:

$$\begin{aligned}
&\text{(a)}\ \sigma = -2(1+2a_{14}/a_{12})p - a_{02}/a_{12},\\
&\text{(b)}\ [a_{01}+a_{02}+(a_{11}+a_{12}+a_{13}+a_{14}+a_{15})\sigma+2(a_{11}+a_{12})p]\\
&\quad [2a_{01}+a_{02}+(2a_{11}+a_{12})\sigma+2(2a_{11}+a_{12}+a_{13}+a_{14}+a_{15})p]\\
&\quad -2[a_{01}+(a_{11}+a_{13})\sigma+(2a_{11}+a_{15})p][a_{01}+(a_{11}+a_{15})\sigma\\
&\quad +(2a_{11}+a_{13})p] = 0,\\
&\text{(c)}\ \sigma = -a_{02}/(a_{12}+a_{14}) - (2a_{12}+a_{14})p/(a_{12}+a_{14}).
\end{aligned} \tag{17}$$

In (17a) and (17b) principal directions of strain rate would be the same as those of stress, but this would not be so for (17c). One possible combination of the failure criteria is shown graphically in Fig. 1. The precise relationship of the three lines in Fig. 1 is, of course, governed by the specific values of the material properties.

Consider now a typical triaxial test in which p is maintained constant while $|\sigma|$ (where $|\sigma| > |p|$) is increased until failure occurs. The typical response is shown in Fig. 2; suppose however, that the test is being run under such conditions that failure is given by the straight line of (17a) in Fig. 1. Failure will then be reached at point A (Fig. 2) at a load less than that given by (17b). The specimen will become instable to shearing motion at point A, and this might be expected to lead to a shear type failure (see Fig. 3). Thus a given material might fail by the mechanism of Fig. 3(a) for one range of pressures and by that of Fig. 3(b) for a different range.

It is of interest to note that a direct analysis of the triaxial test will not investigate instabilities such as (17c).

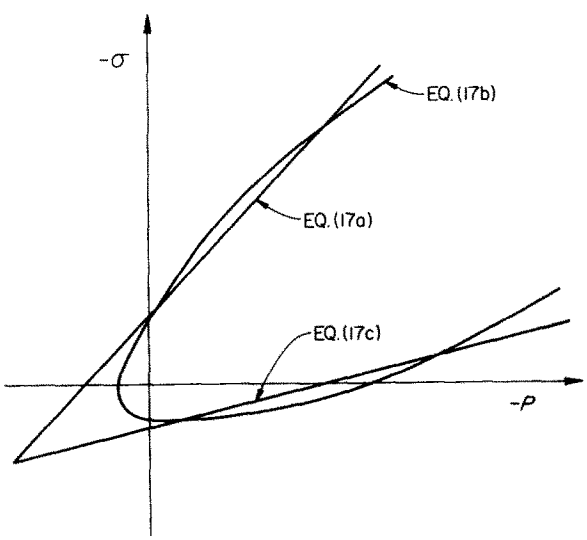

FIG. 1. Representative failure surface for triaxial loading.

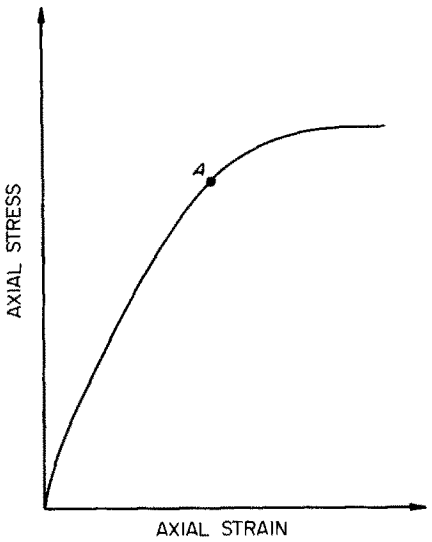

FIG. 2. Representative stress–strain curve.

4. TRIAXIAL BEHAVIOR OF CONCRETE

The behavior of plain concrete in triaxial tests will now be examined using the hypoelastic model. It is certainly true that, in many applications, time dependent aspects of the mechanical response of concrete need to be taken into account [14]. For limited ranges of rate and duration of loading, however, a time independent model is useful. The data which will be utilized [15–18] is for short term loading and will be taken as time independent.

No attempt will be made to make a "best fit" of all available data. The purpose of this section is to demonstrate that the essential features of both the deformation and failure characteristics of a real material are described by the hypoelastic model.

The correlation of test data on plain concrete available in the literature is difficult because the constituents of each researcher's concrete differ slightly. For present purposes the data of Richart *et al.* [15] and Gardner [16] will be utilized. Gardner conducted standard triaxial tests, i.e. tests at constant cell pressure with increasing axial compression and measured both axial and lateral deformations. Richart *et al.* used several different mixes in their triaxial tests. They did not measure lateral deformations, but their data is of particular value with regard to failure considerations because, besides standard tests, they

FIG. 3. Possible failure modes in triaxial test.

also carried out constant cell pressure tests with decreasing axial compression and tests with constant axial compression. Because no information was available by which the mix proportions of the two experimenters might be compared, it was decided to use Richart *et al.*'s data for that mix which gave the best agreement with the data of Gardner.

No unique method exists for determining the hypoelastic constants so they were determined to be consistent with the standard triaxial test data. The following values were chosen

$$\begin{aligned} a_{01} &= 0 \\ a_{02} &= 9 \times 10^5 \text{ psi} \\ a_{11} &= 44 \\ a_{12} &= -88 \\ a_{13} &= -1200 \\ a_{14} &= 0 \\ a_{15} &= -200. \end{aligned} \tag{18}$$

Some discussion of these values is in order. First, the zero value of a_{01} corresponds to zero Poisson's ratio at infinitesimal loads. While, in fact, this number was not quite zero, it was very small. Another constant of particular interest is a_{14}. As may be seen from equation (9), setting this constant equal to zero greatly simplifies the form of the failure criterion and, in addition, renders it dependent only on the invariants I_1 and J_2 and hence symmetric about the hydrostatic stress axis.

Richart's data (see Fig. 4) suggests a small amount of asymmetry about this axis and, in addition, Bresler and Pister [17] have suggested that the failure of concrete is affected

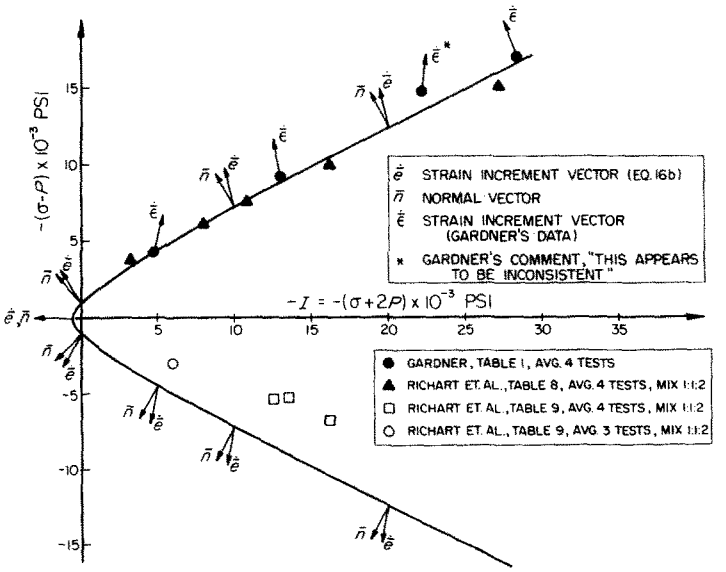

FIG. 4. Failure surface and strain increment vectors for triaxial loading.

by the third invariant of stress. Nevertheless, because of the resulting simplification, a_{14} was taken to be zero. a_{02} was determined from the slope at the origin of the stress–strain curve for zero cell pressure. For computational convenience, the condition $a_{12} = -2a_{11}$ was imposed. The remaining constants a_{11}, a_{13} and a_{15} were found using the failure data of Fig. 4.

The resulting predicted failure line is also shown in Fig. 4. This curve corresponds to equation (17b), the failure lines for (17a) and (17c) both lying outside the curve shown. In addition, strain rate directions predicted by equation (16b) and those measured by Gardner are shown; agreement is good. Also shown are normals to the failure line.

Having determined constants consistent with both initial and ultimate loading, it is now possible to compare predicted and observed behavior over the complete load range. The standard triaxial test data is used for this purpose. Such comparison may be made since, for any prescribed loading path, the hypoelastic constitutive law is integrable. Thus, in the standard triaxial test, because of the constancy of cell pressure,

$$de_2 = -\frac{a_{01}+(a_{11}+a_{15})\sigma+(2a_{11}+a_{13})p}{2a_{01}+a_{02}+(2a_{11}+a_{12})\sigma+2(2a_{11}+a_{12}+a_{13}+a_{14}+a_{15})p}\,de_1 \tag{19}$$

and

$$\begin{aligned}\frac{d\sigma_1}{de_1} = \Big\{&[a_{01}+a_{02}+(a_{11}+a_{12}+a_{13}+2a_{14}+a_{15})\sigma+(2a_{11}+2a_{12})p]\\&[2a_{01}+a_{02}+(2a_{11}+a_{12})\sigma+2(2a_{11}+a_{12}+a_{13}+a_{14}+a_{15})p]\\&-2[a_{01}+(a_{11}+a_{13})\sigma+(2a_{11}+a_{15})p][a_{01}+(a_{11}+a_{13})\sigma\\&+(2a_{11}+a_{13})p]\Big\}/[2a_{01}+a_{02}+(2a_{11}+a_{12})\sigma+2(2a_{11}+a_{12}+a_{13}+a_{14}+a_{15})p].\end{aligned} \tag{20}$$

Using equation (18), equations (19) and (20) may be solved for a given cell pressure. Two cases are computed here.

For zero cell pressure, i.e. the simple compression (or simple tension) test, one obtains

$$\sigma_1 = \frac{-4140[1-e^{1872e_1}]}{1+7{\cdot}62\,e^{1872e_1}} \tag{21a}$$

$$e_2 = -0{\cdot}717[e_1 - 6{\cdot}04\times10^{-4}\ln(1+7{\cdot}62\,e^{1872e_1}) + 1{\cdot}301\times10^{-3}]. \tag{21b}$$

Failure stresses associated with (21a) are $\sigma_1 = -4140$ psi and $\sigma_1 = +540$ psi. Equation (21a) is shown graphically in Fig. 5 together with data from Gardner and Richart *et al.* Gardner's data shows an inflection point which is also indicated by the theory, and it is interesting to note that the theory provides for a limiting value of tension as well as compression at what would seem to be a very realistic value. However, there is no experimental data available to confirm this. As stated above, only Gardner's tests permit lateral deformations to be checked. There is some discrepancy between observed and predicted values (Fig. 6). It should be noted, however, that there was considerable scatter in Gardner's data and that the very small values of the lateral strain make this a difficult quantity to measure.

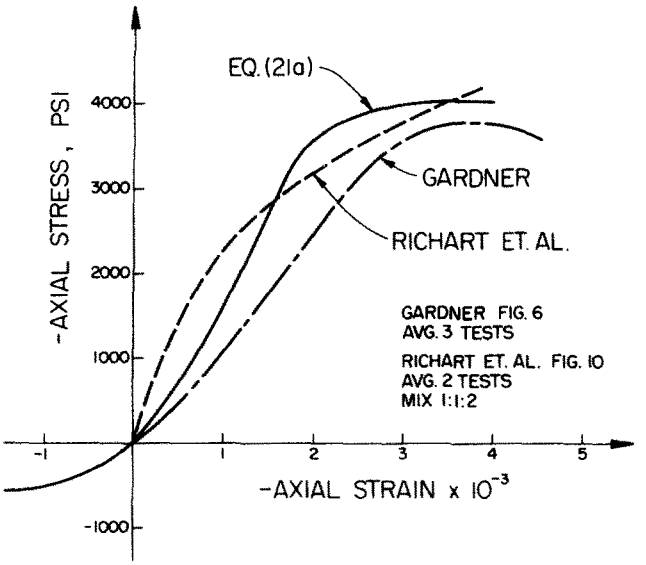

FIG. 5. Stress–strain curve for compression test.

A second example of load–deformation curve has been worked out for the case of a confining pressure of 3750 psi. The results are

$$\sigma_1 - p = \frac{-15{,}550[1 - e^{684e_1}]}{1 + 3\,e^{684e_1}} \tag{22a}$$

$$e_2 = -0{\cdot}587e_1 + 4{\cdot}34 \times 10^{-4} \ln[1 + 3\,e^{684e_1}] - 0{\cdot}601 \times 10^{-3} \tag{22b}$$

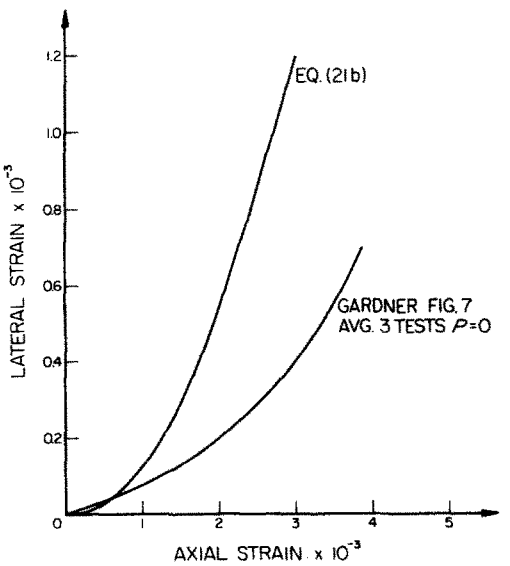

FIG. 6. Lateral vs. axial strain for compression test.

and the graph of these equations together with data are shown in Figs. 7 and 8. In fact, the confining pressure for the two experiments shown in Fig. 7 are not identical, but are very close. Again it should be borne in mind that the theory predicts an infinite amount of

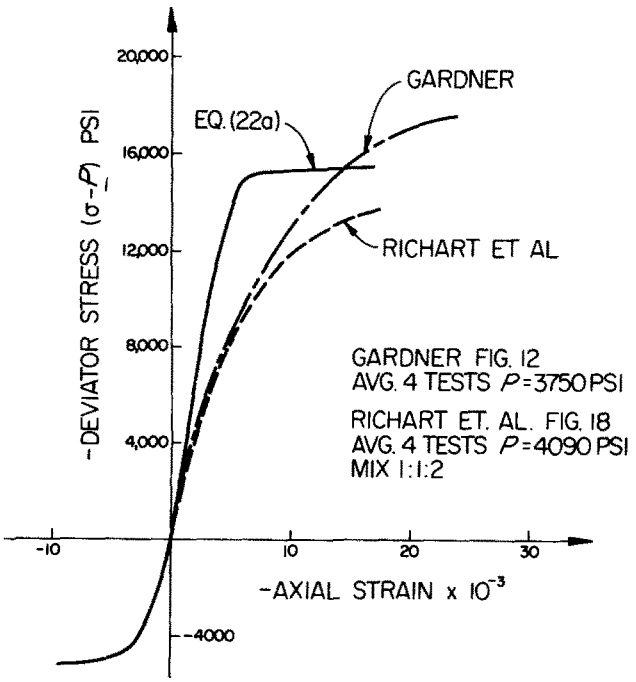

FIG. 7. Deviator stress vs. axial strain for triaxial test.

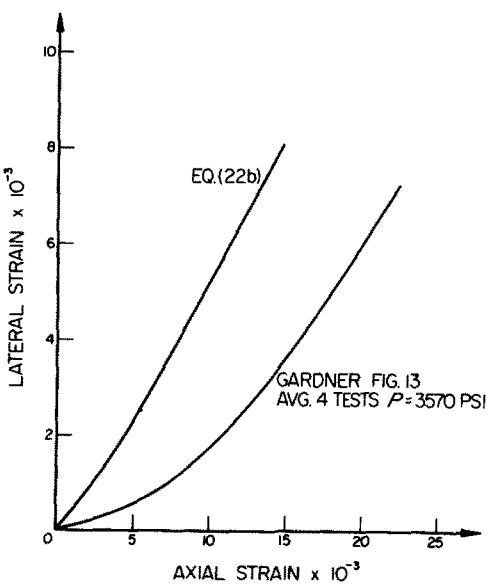

FIG. 8. Lateral vs. axial strain for triaxial test.

deformation before failure is reached. Such deformations are inconsistent with our basic assumptions; however, it can be seen that a very large percentage of the failure load is reached for very small deformations.

5. TORSION–COMPRESSION TESTS ON CONCRETE

An important test of a constitutive law obtained phenomenologically is to show that it gives reasonable predictions for states of stress other than those used to determine material properties. Because Bresler and Pister [17, 18] have examined the failure of thin-walled plain concrete-cylinders under combined torsion and compression, the predicted behavior of the hypoelastic law under such states will be examined.

The state of stress is

$$\sigma_{ij} = \begin{vmatrix} 0 & \sigma_{12} & 0 \\ \sigma_{12} & \sigma_{22} & 0 \\ 0 & 0 & 0 \end{vmatrix} \tag{23}$$

where x_2 is the axis of the cylinder and x_1 lies in the circumferential direction at a typical section.

Thus if L is the length of the cylinder, R its mean radius and t its thickness, the twisting moment M_T and compressive force F are given by

$$M_T = 2\pi R^2 t\sigma_{12}$$

$$F = -2\pi Rt\sigma_{22}.$$

The failure under torsion–compression may be determined directly from (11) which, using (23), becomes

$$(a_{02}+a_{12}\sigma_{22})^4[a_{02}(3a_{01}+a_{02})+\sigma_{22}\{3a_{01}a_{12}+a_{02}(3a_{11}+2a_{12}+a_{13}+a_{15})\}$$
$$+\sigma_{22}^2\{-2a_{13}a_{15}+a_{12}(3a_{11}+a_{12}+a_{13}+a_{15})\}-6a_{13}a_{15}\sigma_{12}^2] = 0 \tag{24}$$

when $a_{14} = 0$. For the constants of (18) this becomes

$$(9\times 10^5 - 88\sigma_{22})^4[8{\cdot}1\times 10^{11} - 1{\cdot}3\times 10^9\sigma_{22} - 3{\cdot}6\times 10^5\sigma_{22}^2 - 1{\cdot}44\times 10^6\sigma_{12}^2] = 0. \tag{25}$$

Limiting failure stresses are, in pure torsion

$$\bar{\sigma}_{12} = 750 \text{ psi}$$

and for axial load only

$$\sigma_{22} = -4140 \text{ psi}$$
$$+540 \text{ psi}.$$

The term $(a_{02}+a_{12}\sigma_{22})$ gives

$$\sigma_{22} = +10{,}200 \text{ psi}$$

and hence, only the right hand term of (24) or (25) governs failure. The value of shear stress predicted seems unreasonably large in comparison with the tensile strength. This essentially arises from taking a_{14} to be zero. A non-zero choice of a_{14} would improve both the tensile

triaxial predictions and the ratio of shear stress to tensile stress but would increase computational work by an order of magnitude.

Bresler and Pister presented their results in non-dimensional form by defining

$$J_2 = 3\tau_0^2$$

$$\tfrac{1}{3}\sigma_{kk} = \sigma_0.$$

Using these values, the right hand term of (25) becomes

$$\left(\frac{\tau_0}{\sigma_c}\right)^2 = 0{\cdot}0218 + 0{\cdot}432\frac{\sigma_0}{\sigma_c} + 0{\cdot}496\left(\frac{\sigma_0}{\sigma_c}\right)^2 \tag{26}$$

where $\sigma_c = -4140$ psi.

This curve is plotted in Fig. 9 together with the experimental results of Bresler and Pister and their proposed linear failure law from [17]

$$-\frac{\tau_0}{\sigma_c} = 1{\cdot}16\frac{\sigma_0}{\sigma_c} + 0{\cdot}086. \tag{27}$$

It may be seen from Fig. 9 that the curve given by (26) is essentially as good a fit to the data as (27). In [18] Bresler and Pister, on the basis of further experimental work, proposed a quadratic law identical in form to (26). Their additional tests indicated lower shear strengths than in [17] and hence the comparison with (26) is slightly poorer.

In addition to obtaining failure data, of course, the hypoelastic law permits load deformation curves to be obtained.

Thus in the torsion–compression test, the state of strain rate may be shown to be

$$\dot{e}_{ij} = \begin{vmatrix} \dot{e}_1 & \dot{e}_{12} & 0 \\ \dot{e}_{12} & \dot{e}_2 & 0 \\ 0 & 0 & \dot{e}_2 \end{vmatrix} \tag{28}$$

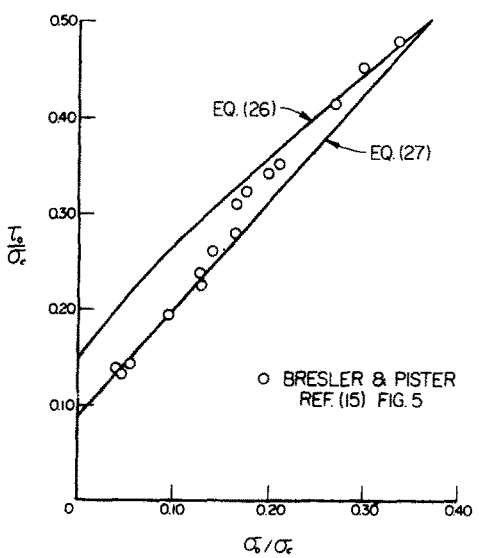

FIG. 9. Failure surface for torsion–compression of hollow cylinder.

when $a_{14} = 0$ and from (2) after eliminating $\dot{e}_1$, one obtains

$$\begin{aligned} d\sigma_{22} = (\{&[a_{02}+\sigma_{22}(a_{11}+a_{12}+a_{13}+a_{15})][a_{02}+(2a_{11}+a_{12})\sigma_{22}] \\ &-2\sigma_{22}^2(a_{11}+a_{13})(a_{11}+a_{15})\}\, de_1+2a_{15}\sigma_{12}[a_{02} \\ &+(a_{12}-a_{13})\sigma_{22}]\, de_{12})/[a_{02}+(2a_{11}+a_{12})\sigma_{22}] \end{aligned} \tag{29}$$

$$\begin{aligned} d\sigma_{12} = \{&a_{12}\sigma_{12}[a_{02}+(a_{12}-a_{15})\sigma_2]\, de_1+[a_{02}^2+2a_{02}(a_{11}+a_{12})\sigma_{22} \\ &+a_{12}(2a_{11}+a_{12})\sigma_{22}^2-4a_{13}a_{15}\sigma_{12}^2]\, de_{12}\}/[a_{02}+(2a_{11}+a_{12})\sigma_{22}] \end{aligned} \tag{30}$$

when $a_{01} = a_{14} = 0$ and $a_{12} = -2a_{11}$.

These equations may be solved for prescribed loading paths of σ_{22} and σ_{12}. In particular, for the torsion test, i.e. $\sigma_{22} = 0$, (29) and (30) may be solved to give

$$e_{12} = \frac{1}{2\sqrt{6a_{13}a_{15}}} \ln \left| \frac{a_{02}+\sqrt{6a_{13}a_{15}}\sigma_{12}}{a_{02}-\sqrt{6a_{13}a_{15}}\sigma_{12}} \right| \tag{31}$$

and

$$e_1 = \frac{1}{6a_{13}} \ln \left| 1-\frac{6a_{13}a_{15}\sigma_{12}^2}{a_{02}^2} \right|. \tag{32}$$

In the above, the initial conditions used were zero deformation at zero load.

The stress–strain curves given by (31) and (32) are plotted in Fig. 10. Because Bresler and Pister did not measure deformations, no comparison with experimental data is possible.

6. CONCLUSIONS

The theory presented in this paper may be regarded as a convenient representation of physically nonlinear behavior. The advantage of the hypoelastic representation is that a single constitutive law fulfills two purposes: for prescribed loading paths, stresses and

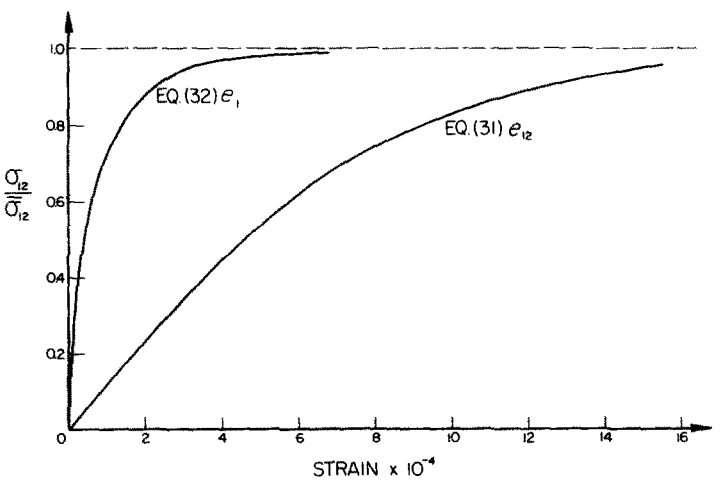

FIG. 10. Stress–strain curves for the torsion of hollow cylinders.

deformations may be obtained up to and including failure; in addition, a direct determination of limiting or failure states is possible.

As a particular application, the behavior of plain concrete has been considered. Material constants have been determined from initial and limiting triaxial behavior. The resulting law describes well the complete triaxial behavior and also agrees reasonably with available failure data for combined torsion and compression.

REFERENCES

[1] C. TRUESDELL, Hypo-elasticity. *J. ration. Mech. Analysis* **4**, 83–133, 1019–1020 (1955).
[2] C. TRUESDELL, Hypo-elastic shear. *J. appl. Phys.* **27**, 441–447 (1956).
[3] A. E. GREEN, Hypo-elasticity and plasticity. *Proc. R. Soc. Lond.* **A234**, 46–57 (1956).
[4] A. E. GREEN, Hypo-elasticity and plasticity II. *J. ration. Mech. Analysis* **5**, 725–734 (1956).
[5] M. D. COON and R. J. EVANS, On the recoverable deformation of granular media. *Am. Soc. civ. Engrs Soil Mech.* to appear.
[6] R. J. EVANS and K. S. PISTER, Constitutive equations for a class of nonlinear elastic solids. *Int. J. Solids Struct.* **2**, 427–445 (1966).
[7] D. C. DRUCKER and W. PRAGER, Soil mechanics and plastic analysis or limit design. *Q. appl. Math.* **10**, 157–165 (1952).
[8] R. HILL, New horizons in the mechanics of solids. *J. Mech. Phys. Solids* **5**, 66–74 (1956).
[9] D. C. DRUCKER, A More Fundamental Approach to Plastic Stress–Strain Relations, *Proc. 1st. U.S. Nat. Cong. Appl. Mech.*, pp. 487–991 (1951).
[10] G. DE JOSSELIN DE JONG, Lower Bound Collapse Theorem and Lack of Normality of Strain Rate to Yield Surface for Soils, *IUTAM Symposium on Rheology and Soil Mechanics*, Grenoble, pp. 69–78 (1964).
[11] R. M. HAYTHORNTHWAITE, Stress and Strain in Soils, Plasticity, *Proc. 2nd Symp. Naval Struct. Mech.*, Brown University, pp. 185–193. Pergamon Press (1960).
[12] A. C. PALMER, A limit theorem for materials with non-associated flow laws. *J. Méc.* **5**, 217–222 (1966).
[13] Z. MROZ, Non-associated flow laws in plasticity. *J. Méc.* **2**, 21–42 (1963).
[14] J. L. SACKMAN, Creep of Concrete and Concrete Structures, *Proc. Princeton University Conference on Solid Mechanics*, Princeton, New Jersey, pp. 15–48 (1963).
[15] F. E. RICHART, A. BRANDTZAEG and R. L. BROWN, A Study of the Failure of Concrete under Combined Compressive Stresses, *Univ. Ill. Eng. Exp. Station*, Bull. No. 185, p. 104 (1928).
[16] N. J. GARDNER, Triaxial behavior of concrete. *ACI Jl Proc.* **66**, 136–146 (1969).
[17] B. BRESLER and K. S. PISTER, Failure of plain concrete under combined stresses. *Trans. Am. Soc. civ. Engrs.* **22**, 1049–1059 (1957).
[18] B. BRESLER and K. S. PISTER, Strength of concrete under combined stresses. *ACI Jl Proc.* **55**, 321–346 (1958).

(*Received* 16 *January* 1971; *revised* 12 *October* 1971)

Абстракт—Исследуется конститутивный закон приращения, независящего от времени, соответствующий гипоупругости, при особенным отношении оге описа разрушения. Определяются постоянные материала для обыкновенного бетона. Указано, что суммарный закон описывает поведение до время разрушения и самое разрушение для трехосного и комбинированного кручения и сжимаемой нагрузки.